Journal Website: https://www.icjn.net/jhpap ISSN: 3136-1927 | EISSN: 3136-1935

Journal of High Performance Alloys and Processing (JHPAP)

ICJN Press Volume. 01 | Issue. 01 | Oct. 2026 DOI: 10.66729/jhpap202603017



ARTICLE

Effect of Cryogenic Treatment on the Friction and Wear Properties of GCr15 Bearing Steel

Chang Ren[1], Qingfeng Ding[1,2*], Jiaming Li[1], Hao Tian[2], Chengfu Duan[1]

1 Department of Automotive Materials, Hubei University of Automotive Technology, Shiyan Hebei 442002, China.
2 Department of Bearing Steel Research Laboratory, Hubei Key Laboratory of High-Quality Specialty Steel, Huangshi Hebei 435001, China.

*Corresponding Author: Qingfeng Ding, E-mail: 20220057@huat.edu.cn

Abstract

The effects of different cryogenic treatment durations on the microstructure and properties of GCr15 bearing steel were investigated through performance testing, friction and wear tests, X-ray diffraction (XRD), and scanning electron microscope (SEM). The results indicate that after cryogenic treatment, the content of fine carbides increases and they are more uniformly dispersed, while the amount of retained austenite is reduced. Compared to the non-cryogenically treated sample, the retained austenite content decreases by 27% and 39.20% after 6 h and 72 h of cryogenic treatment, respectively. Consequently, the hardness and wear resistance of GCr15 bearing steel are enhanced following cryogenic treatment, and prolonging the cryogenic duration is beneficial for further improving its performance. When the cryogenic time is extended from 6 h to 72 h, the hardness increases from 684.60 HV1.0 to 690.80 HV1.0 and then to 701.20 HV1.0; the wear rate decreases from 5.87×10^{-6} mm^3/(N·m) to 4.45×10^{-6} mm^3/(N·m) and then to 2.95×10^{-6} mm^3/(N·m), respectively. Compared with the non-cryogenically treated D0 sample, the wear rate of the D2 sample (cryogenically treated for 72 h) was reduced by 49.70%, exhibiting the optimal wear resistance.

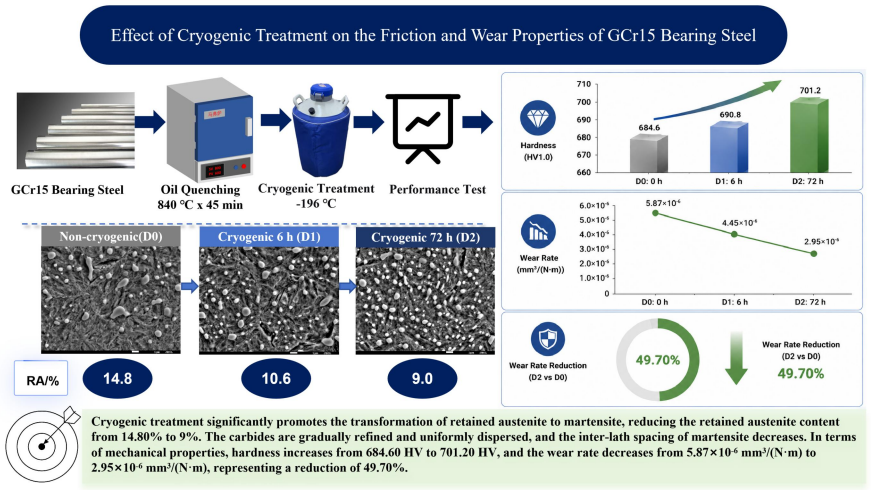
Keywords

GCr15 bearing steel; Cryogenic time; Microstructure; Hardness; Friction and wear propertie

Citation: Chang Ren, Qingfeng Ding, Jiaming Li, *et al*. Effect of Cryogenic Treatment on the Friction and Wear Properties of GCr15 Bearing Steel. *Journal of High Performance Alloys and Processing*. 2026, 01 (1): 1-9. doi: 10.66729/jhpap202603017.

Copyright:© 2026 The Author(s). Published by ICJN Press.
This is an open access article under the https://creativecommons.org/licenses/by/4.0/
Received 17 March 2026; Revised 13 April 2026; Accepted 5 June 2026; Available online 31 October 2026.

Graphical Abstract



Highlights

- Cryogenic treatment at -196 °C significantly reduces retained austenite in GCr15 bearing steel by up to 39.20%.
- Prolonged cryogenic treatment refines carbides and promotes uniform dispersion within the martensitic matrix.
- Hardness increases by 2.40% and wear rate decreases by 49.70% after 72 h cryogenic treatment.
- Cryogenic treatment offers a cost-effective approach to enhance bearing steel performance.

1. Introduction

As a fundamental structural material, bearing steel is widely used in high-speed, heavy-load, and high-precision mechanical transmission systems, and its service performance determines the reliability and operational lifespan of the equipment[1]. The long-established high-carbon chromium bearing steel GCr15, owing to its conventional heat treatment process involving oil quenching and low-temperature tempering, develops a martensitic microstructure that endows bearings with high hardness, excellent wear resistance, and good fatigue properties[2]. Consequently, this bearing material has been extensively applied since its inception. However, following conventional heat treatment, a certain amount of retained austenite and coarse carbides persists within the material. This not only limits further improvements in its hardness and wear resistance but also constrains its service life under extreme operating conditions[3,4]. Therefore, the development of novel and efficient heat treatment processes to optimize the microstructure of GCr15 bearing steel, and thereby enhance its properties, holds significant theoretical research value and engineering application prospects.

Cryogenic treatment, recognized as a simple, cost-effective, and non-polluting method for improving the mechanical properties of materials, has recently been confirmed to effectively regulate the microstructure and performance of steels[5,6]. It is progressively becoming an integral part of conventional heat treatment routines. Research[7] indicates that cryogenic treatment can not only significantly reduce the retained austenite content in high-alloy steels after heat treatment but also enhance their hardness, toughness, and wear resistance, serving as an important means to extend the service life of components. Cryogenic process parameters directly influence the transformation of retained austenite and microstructural evolution. Optimizing the cryogenic treatment process is an effective approach to obtaining materials with superior performance[8,9]. Current research on the cryogenic treatment of GCr15 bearing steel primarily focuses on comparisons between different heat treatment processes[10,11] and the effect of processing sequence[12,13] on the material's microstructure and properties. Studies on the influence of cryogenic time[14] on GCr15 bearing steel are relatively limited. In particular, there is a lack of in-depth, quantitative analysis and theoretical elucidation concerning the intrinsic correlation mechanisms between cryogenic time and the evolution of microstructure, hardness, and wear resistance improvement in this steel.

This study investigates GCr15 bearing steel subjected to various cryogenic treatment durations. Through comparative analysis of microstructural observation, hardness testing, and friction and wear performance, the effects of different cryogenic times on the material's microstructure, hardness, wear rate, and wear mechanisms were systematically studied. The findings aim to provide a reference for optimizing the cryogenic treatment process for GCr15 bearing steel.

2. Material and Methods

The experimental material was an as-annealed GCr15 steel bar with a diameter of 30 mm, and its chemical composition range is listed in **Table 1.**

Table 1. Chemical composition of GCr15 bearing steel mass fraction (%)

C	Si	Mn	P	S	Cr	O
1.02	0.25	0.34	0.008	0.0008	1.42	0.0005

Figure 1 shows the schematic diagram of the whole experimental procedure. As illustrated, the bar stock was cut into cylinders measuring φ30 × 20 mm and subsequently subjected to austenitizing treatment in a KSL-1200X box-type (Hefei Kejing Materials Technology Co., Ltd., Hefei, China) resistance furnace. The specimens were austenitized at 840 °C, held for 45 min, and then oil-cooled. Following quenching, the specimens were subjected to cryogenic treatment for different durations. The cryogenic treatment was performed in liquid nitrogen at -196 °C, with holding times of 0 h, 6 h, and 72 h. Thereafter, all specimens were tempered at 180 °C and designated as D0, D1, and D2, respectively.

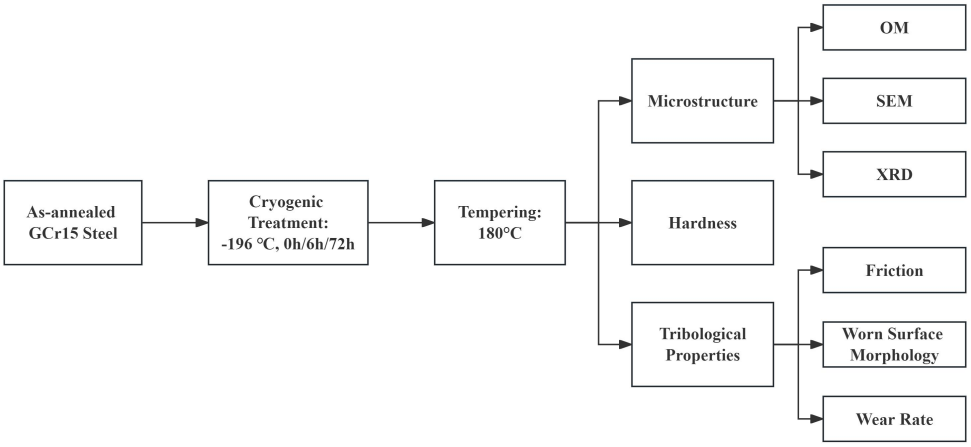


Figure 1. Schematic diagram of the experimental procedure. **NOTE:** OM: Optical Microscope; SEM: Scanning Electron Microscope; XRD: X-ray Diffraction. Copyright: Drawn by the authors using Microsoft PowerPoint, version 2013.

After tempering, the specimens were machined into small blocks of 20 mm × 10 mm × 5 mm. Rockwell hardness was measured using a TouchRock 150 pro digital Rockwell (Shanghai Hengyi Precision Instrument Co., Ltd., Shanghai, China) hardness tester, with five measurements taken per specimen and the average value reported. Microhardness was measured using an MH-500 digital microhardness (Shanghai Hengyi Precision Instrument Co., Ltd., Shanghai, China) tester under a load of 1,000 g with a dwell time of 15 s; five indentations were made on each specimen, and the average value was taken as the hardness under the corresponding processing condition. The microstructure of the base material was observed by optical microscopy (Carl Zeiss AG, Oberkochen, Germany) after etching with 4 vol% nitric acid in ethanol. Phase identification was conducted using a SmartLab SE X-ray diffractometer (Rigaku Corporation, Tokyo, Japan), and the retained austenite content was quantitatively analyzed. The microstructure was further examined using a 7900F high-resolution field-emission (JEOL Ltd., Tokyo, Japan) scanning electron microscope.

Friction and wear tests were performed using an MFT-5000 multifunctional tribometer (Rtec Instruments, San Jose, CA, USA). A ball-on-disk linear reciprocating mode was adopted, with a Si_3N_4 counterbody ball (diameter: 6.35 mm, hardness > 1,400 HV) as the mating material. The test parameters were set as follows: reciprocating stroke of 15 mm, sliding speed of 5 mm/s, normal load of 150 N, and test duration of 30 min. After the wear tests, the specimens were cleaned with alcohol. The three-dimensional topography of the worn surfaces and the wear scar volume were characterized using a VT6100 laser confocal microscope (Shenzhen Chotest Technology Co., Ltd., Shenzhen, China). Wear morphology was observed using a JSM-6510LV scanning electron microscope (JEOL Ltd., Tokyo, Japan), and the chemical elements on the wear scars were analyzed using its attached energy-dispersive spectrometer. The wear rate for specimens under different cryogenic durations was calculated by substituting the relevant wear test data into Equation (1).

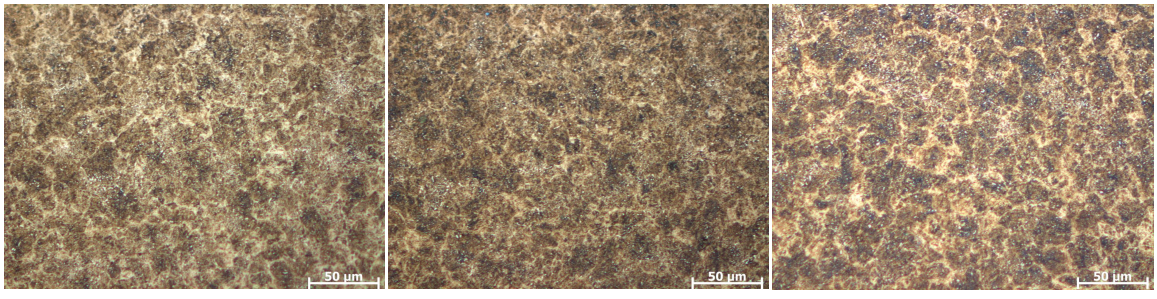
$$\sigma = \frac{V}{\sum W} \quad (1)$$

Where σ is the wear rate (in $mm^3/(N \cdot m)$), V is the wear volume of the specimen (in mm^3), and W is the cumulative friction work (in N·m).

3. Results and Discussion

3.1 Microstructure

The microstructure of GCr15 bearing steel after different cryogenic treatment durations and subsequent tempering is shown in the **Figure 2**.

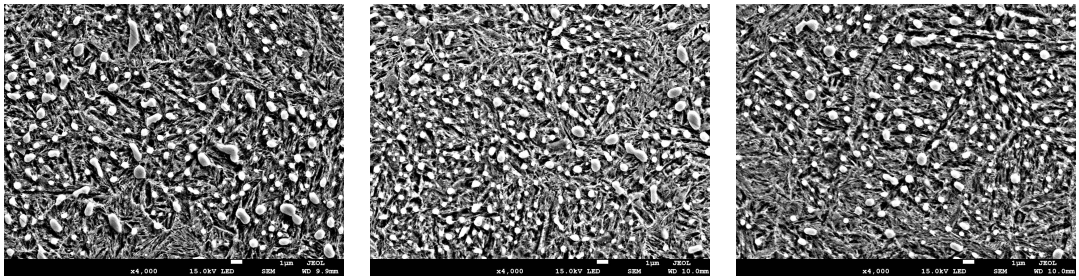


(a) (b) (c)

Figure 2. Microstructure of GCr15 bearing steel after different cryogenic times and tempering. (a) D0 : no cryogenic treatment; (b) D1: cryogenic treatment for 6 hours.; (c) D2: cryogenic treatment for 72 h. Scale bar: 50 μm. Copyright: This image was captured by OM, Zeiss metallographic microscope.

Figure 2(a) shows the microstructure of the D0 specimen, which was quenched and tempered at 180 ℃ without cryogenic treatment. The microstructure consists primarily of tempered martensite, retained austenite, and carbides. **Figure 2(b)** presents the microstructure of the D1 specimen subjected to 6 h of cryogenic treatment followed by tempering at 180 ℃. The cryogenic process significantly promoted the transformation of retained austenite to martensite and catalyzed the precipitation of carbides[15]. Consequently, the carbide distribution in this specimen is finer and more dispersed compared to that of D0. **Figure 2(c)** displays the microstructure of the D2 specimen after 72 h of cryogenic treatment and subsequent tempering at 180 ℃. The prolonged cryogenic duration facilitated the most complete microstructural transformation, reducing the retained austenite content to its minimum and forming highly dispersed fine carbides.

To further investigate the influence mechanism of cryogenic duration on the microstructure of GCr15 bearing steel, the specimens were observed using scanning electron microscopy (SEM), as shown in the **Figure 3**.



(a) (b) (c)

Figure 3. SEM images of GCr15 bearing steel after different cryogenic times and tempering. (a) D0: no cryogenic treatment; (b) D1: cryogenic treatment for 6 hours; (c) D2: cryogenic treatment for 72 h. Scale bar: 1 μm. Copyright: This image was captured by SEM, 7900F high-resolution field-emission scanning electron microscope.

Comparative analysis reveals that the specimens subjected to cryogenic treatment exhibit distinct martensite lath morphology within the matrix, with a higher content of precipitated carbides compared to those processed by conventional heat treatment. In the cryogenically treated specimens D1 and D2, the precipitation of fine carbides increases, and retained austenite is transformed into martensite, resulting in an increased martensite content and microstructural refinement. With prolonged cryogenic duration, the transformation of retained austenite to martensite becomes more complete in specimen D2. Carbon elements within the microstructure tend to segregate between martensite laths[16,17], thereby promoting the precipitation of numerous fine and uniformly distributed carbides within the matrix and reducing the inter-lath spacing of martensite.

3.2 XRD

Figure 4 shows the X-ray diffraction (XRD) patterns of GCr15 bearing steel after different cryogenic treatment durations and subsequent tempering.

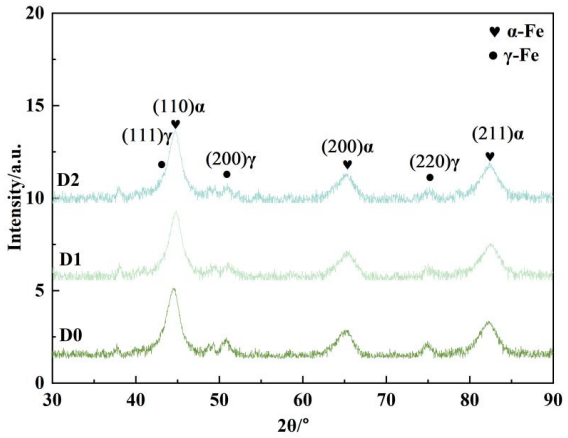


Figure 4. XRD patterns of GCr15 bearing steel after different cryogenic times and subsequent tempering. **NOTE:** 2θ/°: the diffraction angle 2θ. Copyright: Drawn by the authors using Origin, version 2024.

The D0 specimen exhibited distinct diffraction peaks for α-Fe and austenite. After cryogenic treatment, the D1 and D2 specimens showed a significant increase in the intensity of α-Fe diffraction peaks, while the austenite peaks became considerably weaker. In the D2 specimen, only a minor protrusion of the austenite peak remained.

The retained austenite volume fraction was calculated by the direct comparison method according to X-ray diffraction intensity theory:

$$C_\gamma = \frac{(I_\gamma/R_\gamma)}{(I_\gamma/R_\gamma)+(I_\alpha/R_\alpha)} \times 100\% \quad (3-1)$$

Where C_γ is the retained austenite volume fraction (%), R_γ and R_α are the integrated and theoretical intensities of γ-Fe peaks, I_γ and I_α are those of α-Fe peaks. The (200)γ, (220)γ, and (111)γ austenite peaks and the (200)α, (211)α martensite peaks were used, and the average value from multiple peaks was adopted. The volume fraction of retained austenite calculated from the XRD patterns is presented in **Table 2**.

Table 2. Results of the calculated retained austenite content in the specimen

No.	Retained Austenite Content/%
D0	14.80
D1	10.60
D2	9

As shown in **Table 2**, compared with the non-cryogenically treated specimen, the retained austenite content in the D1 and D2 specimens subjected to 6 h and 72 h of cryogenic treatment decreased by 27% and 39.20%, respectively. Therefore, the retained austenite content after cryogenic treatment is significantly lower than that obtained by conventional heat treatment processes. This indicates that the substantial decrease in ambient temperature during cryogenic treatment induces volume contraction of martensite, thereby reducing the internal compressive stress within the material[18]. Consequently, the transformation of retained austenite to martensite proceeds continuously, leading to a reduction in retained austenite content. Among all specimens, the D2 specimen subjected to 72 h of cryogenic treatment exhibited the lowest retained austenite content.

3.3 Hardness

Figure 5 presents the hardness results of GCr15 bearing steel after different cryogenic treatment durations and subsequent tempering.

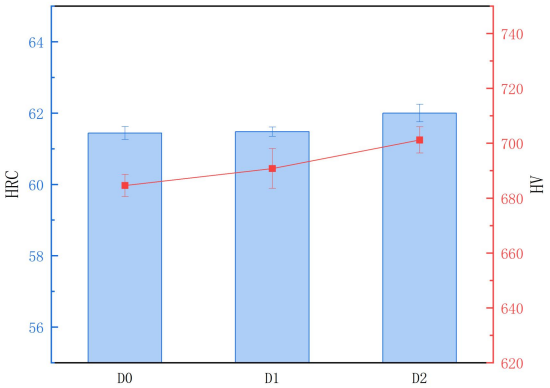


Figure 5. Hardness results of GCr15 bearing steel after different cryogenic times and subsequent tempering. **NOTE:** HRC: Rockwell Hardness (scale C); HV: Vickers Hardness. Copyright: Drawn by the authors using Origin, version 2024.

As shown in the figure, the hardness of GCr15 bearing steel gradually increases with prolonged cryogenic duration, reaching a maximum value at 72 h, from 684.60 HV1.0 to 701.20 HV1.0. The cryogenic temperature provides the driving force for the transformation of retained austenite to martensite. During this transformation, volume expansion and lattice distortion occur, generating significant internal stresses within the material[19,20]. These internal stresses further enhance the hardness by inhibiting dislocation motion. Following cryogenic treatment, the transformation of retained austenite to martensite strengthens the matrix microstructure and improves microstructural homogeneity. Furthermore, cryogenic treatment promotes the dispersed precipitation of carbides, enhancing precipitation strengthening. Therefore, the hardness of GCr15 bearing steel increases after cryogenic treatment.

3.4 Tribological Properties

3.4.1 Friction

Figure 6 shows the instantaneous friction coefficient of GCr15 bearing steel during friction and wear testing after different cryogenic treatment durations and subsequent tempering. **Figure 7** presents the corresponding average friction coefficient.

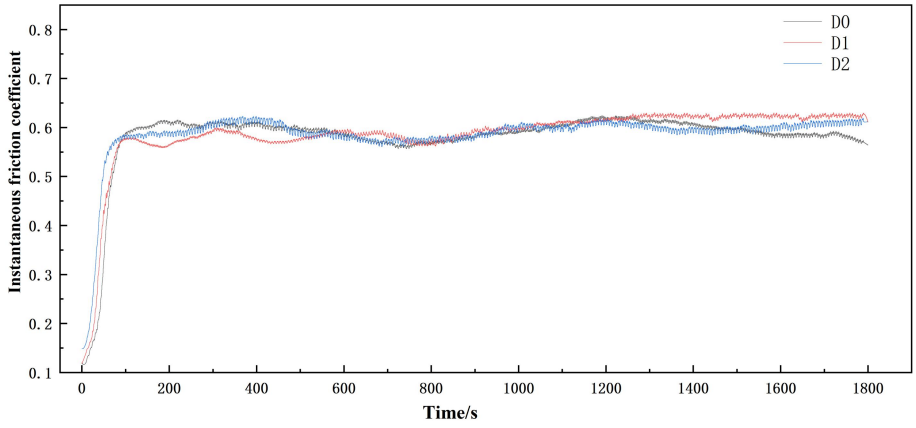


Figure 6. Instantaneous friction coefficient. Copyright: Drawn by the authors using Origin, version 2024.

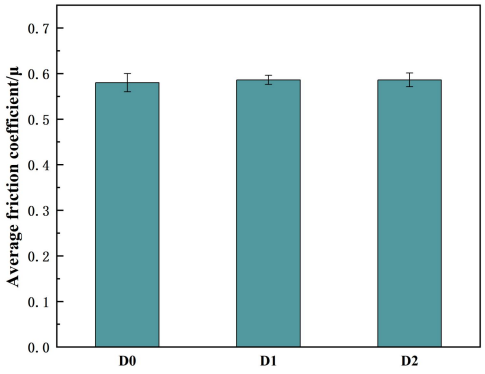


Figure 7. Average friction coefficient. Copyright: Drawn by the authors using Origin, version 2024.

As shown in the **Figure 6**, after a brief running-in period, the friction coefficient of all specimens initially stabilized rapidly. This is attributed to the establishment of good contact between the specimen and the counterbody ball after the running-in stage, leading to a stable friction coefficient[21]. As sliding progressed, the friction coefficients of the D0 and D2 specimens fluctuated within a certain range and then gradually decreased before eventually stabilizing. In contrast, the friction coefficient of the D1 specimen, after fluctuating within a similar range, began to increase slowly and then stabilized. Overall, the instantaneous friction coefficients of the D1 and D2 specimens exhibited smaller fluctuations, while that of the D0 specimen showed greater variability.

As shown in the **Figure 7,** the average friction coefficients of the D0, D1, and D2 specimens were 0.580, 0.586, and 0.586, respectively. Compared with the non-cryogenically treated D0 group, the average friction coefficients of the cryogenically treated D1 and D2 groups increased slightly, with an increment of only about 1%, indicating a negligible difference.

3.4.2 Worn Surface Morphology

Figure. 8 presents the three-dimensional topography of wear scars on GCr15 bearing steel specimens after different cryogenic treatment durations and subsequent tempering. It can be observed that under continuous sliding and compression by the Si_3N_4 ball, distinct wear scar contours formed on the surface of all three specimen.

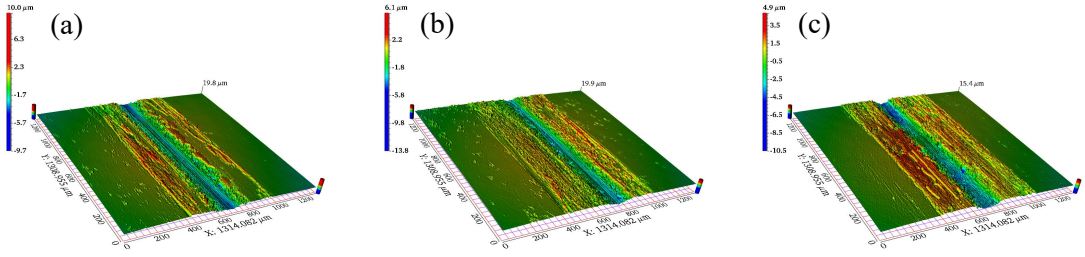


Figure 8. Three-dimensional (3D) wear morphologies after the test. (a) D0; (b) D1; (c) D2. Copyright: This image was captured by VT6100 laser confocal microscope.

Figure 9 shows the profile measurement dimensions of the worn surfaces of the three specimens under a load of 150 N. The results indicate that the D0 specimen exhibited uneven furrow depth distribution and the most severe surface damage, with both the width and depth of the wear scar being greater than those of the other two specimens. The maximum pit depth of this specimen was -0.381 μm. The D1 specimen showed reduced wear scar width and depth compared to D0, with a maximum pit depth of -0.317 μm. The D2 specimen displayed the least surface damage, with the smallest wear scar width and depth, and a maximum pit depth of -0.283 μm. Therefore, based on the evolution of wear scar dimensions, the surface wear resistance of GCr15 bearing steel progressively improves with increasing cryogenic duration.

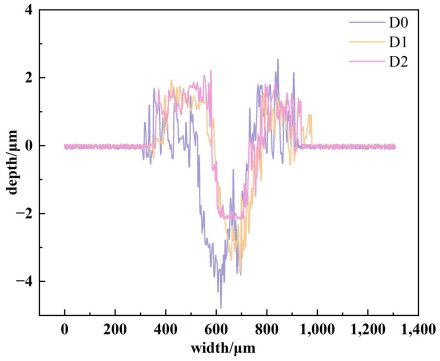


Figure 9. Measured profile dimensions of the wear scar. Copyright: Drawn by the authors using Origin, version 2024.

Figure 10 shows the microstructure and O elemental distribution at the valley bottom **Figure 10(a1–c1)** and sidewall **Figure 10(a2–c2)** of wear scars on GCr15 bearing steel specimens after different cryogenic treatment durations and subsequent tempering. **Table 3** presents the EDS area scanning results of the entire worn region at both the valley bottom and sidewall.

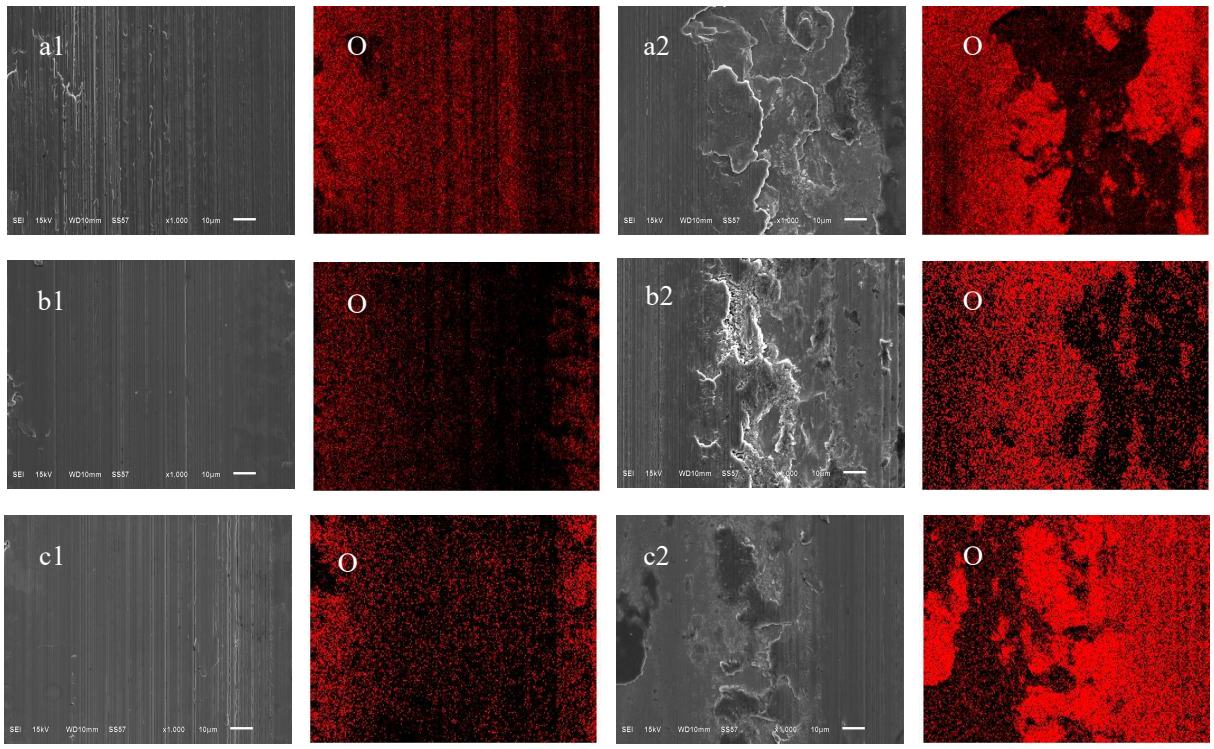


Figure 10. Microstructure and EDS elemental distribution at the bottom and sidewall of the wear scar. (a1) the valley bottom-D0; (a2) sidewall-D0; (b1) the valley bottom-D1; (b2) sidewall-D1; (c1) the valley bottom-D2; (c2) sidewall-D2; (O) O elemental distribution. Scale bar: 10 μm. Copyright: This image was captured by SEM, JSM-6510LV scanning electron microscope.

Table 3. Surface scan Energy Dispersive X-ray Spectroscopy of the worn morphology of the valley bottom and sides after wear (mass fraction, %)

Area	C	O	Si	Cr	Fe
a1	0.25	12.34	1.07	1.29	85.05
b1	0.25	11.86	1.29	1.33	85.27
c1	0.23	11.16	1.13	1.38	86.09
a2	0.40	19.71	2.17	1.19	76.53
b2	0.30	17.19	2.28	1.21	79.02
c2	0.35	16.73	1.73	1.25	79.94

Combining the results from the **Figure 10** and **Table 3**, slight O element enrichment was detected at some furrow locations on the wear scar valleys, indicating the formation of a thin oxide film on the furrow surfaces during the friction and wear process. Therefore, the valley bottoms are primarily characterized by abrasive wear and oxidative wear, accompanied by minor adhesive wear. In contrast, the sidewalls of the wear scars are dominated by adhesive wear and oxidative wear. The non-cryogenically treated D0 specimen exhibited the most severe wear. The valley bottom **Figure 10(a1)** displayed distinct, deep parallel furrows, with pits, and some adhered wear debris was observed on the furrows. Localized material spalling was also evident. The sidewall **Figure 10(a2)** showed features of adhesive and oxidative wear, indicating poor wear resistance of this specimen. For the D1 specimen subjected to 6 h of cryogenic treatment, the furrows at the valley bottom **Figure 10(b1)** became significantlyshallower and finer. Material spalling and adhesion were substantially reduced, and the surface appeared relatively smooth, indicating effective mitigation of wear damage. The sidewall **Figure 10(b2)** exhibited adhesive and oxidative wear, with alower oxygen content, suggesting that cryogenic treatment effectively inhibited oxidation reactions during wear and significantly improved wear resistance. For the D2 specimen subjected to 72 h of cryogenic treatment, the valley bottom **Figure 10(c1)** showed minimal pits and wear debris on the furrows, with notably reduced oxidative wear areas and a relatively smooth and flat surface. The sidewall **Figure 10(c2)** displayed adhesive and oxidative wear, with the lowest oxygen content among all specimens, indicating the best wear resistance.

In summary, cryogenic treatment reduces the presence of large carbides, thereby minimizing wear spalling on the surface under load. Simultaneously, it increases the number of fine carbides, and these

uniformly dispersed fine carbides effectively strengthen the matrix, contributing to improved wear resistance[22–24]. With prolonged cryogenic duration, the quantity of large carbides further decreases while the precipitation of fine carbides increases, thereby progressively enhancing the wear resistance of GCr15 bearing steel.

3.4.3 Wear Rate

Figure 11 presents the wear rate of GCr15 bearing steel specimens after different cryogenic treatment durations and subsequent tempering. The results show that the non-cryogenically treated D0 specimen exhibited the highest wear rate of 5.87 × 10^{-6} $mm^3/(N·m)$. With increasing cryogenic duration, the wear rates of the D1 and D2 specimens gradually decreased to 4.45 × 10^{-6} $mm^3/(N·m)$ and 2.95 × 10^{-6} $mm^3/(N·m)$, respectively. Compared with the D0 specimen, the wear rate of the D2 specimen was reduced by 49.70%, demonstrating the optimal wear resistance, which is consistent with the wear morphology observations.

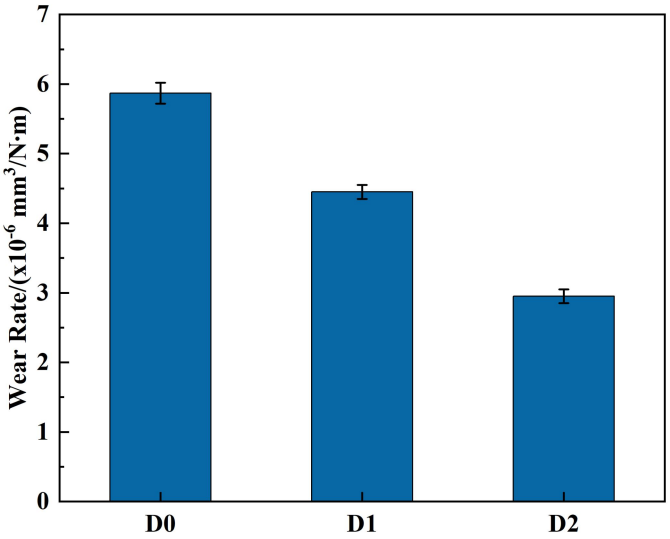


Figure 11. Comparison of wear rates after different cryogenic treatment durations. Drawn by the authors using Origin, version 2024.

It is suggested that the improved wear resistance of the cryogenically treated specimens can be attributed to the increased quantity and number density of fine carbides, as well as the reduction in retained austenite content[25]. These microstructural changes contribute to a significant increase in material hardness, thereby more effectively reducing the wear rate. Furthermore, the fine carbides distributed on the wear surface promote early fracture of wear debris during the friction process, reducing debris size and consequently minimizing material loss[26].

4. Conclusions

This study investigated the effects of different cryogenic treatment durations at -196 ℃ on the microstructure, hardness, wear rate, and wear mechanisms of GCr15 bearing steel. The results were compared and analyzed, leading to the following conclusions:

(1) Cryogenic treatment at -196 ℃ significantly refines the microstructure of GCr15 bearing steel by promoting retained austenite to martensite transformation and inducing fine, uniformly dispersed carbide precipitation. Retained austenite was reduced by 27% (6 h) and 39.20% (72 h) compared with the untreated condition.

(2) Prolonged cryogenic treatment enhances hardness monotonically. Surface hardness increased from 684.60 HV1.0 (6 h) to 701.20 HV1.0 (72 h), due to martensitic strengthening and carbide refinement.

(3) Wear resistance improves markedly with increasing cryogenic duration. The wear rate decreased from 5.87 × 10^{-6} $mm^3/(N·m)$ (untreated) to 2.95 × 10^{-6} $mm^3/(N·m)$ after 72 h, corresponding to a 49.70 % reduction and indicating optimal wear performance at prolonged cryogenic exposure.

As discussed, this study only investigated a limited set of cryogenic durations, and the wear mechanism analysis lacked surface chemical characterization such as X-ray Photoelectron Spectroscopy (XPS). Moreover, the results obtained under laboratory conditions require further validation on actual bearing components. These constraints should be considered when generalizing the findings.

Author Contributions

Concptualization, Qingfeng Ding; methodology, Qingfeng Ding and Hao Tian; validation, Jiaming Li and Chengfu Duan; formal analysis, Chang Ren; investigation, Chang Ren and Jiaming Li; resources, Qingfeng Ding and Hao Tian; writing — original draft preparation, Chang Ren; writing — review and editing: Chang Ren and Qingfeng Ding.

Data Availability

The data supporting the findings of this study are available from the corresponding author upon reasonable request.

Acknowledgments

The authors declare that no specific acknowledgements are required.

Conflicts of Interest

The authors declare no competing financial interests.

Funding

This work was supported by the Major Research Project of Hubei Province (JD) (Grant No. 2023BAA019).

References

[1] Qingkai Han, Baogang Wen, Yufei Guo, *et al.* Technical Evolution of High Power Wind Turbine Bearings. *Bearing*. 2023, (6): 1-13. [Google Scholar] [DOI] (in Chinese)

[2] Songze Zhou, Xiaofeng Wang, Jianfu Chen, *et al.* Effect of low temperature tempering time on microstructure evolution and mechanical properties of GCr15 steel. *Transactions of Materials and Heat Treatment*. 2021, 42 (5): 64-71. [Google Scholar] [DOI](in Chinese)

[3] Zhengxu Li, Jie Deng, Feng Wang. Influence of retained austenite state on wear resistance of GCr15 bearing steel. *China Metallurgy*. 2025, 35 (10): 49-61. [DOI] (in Chinese)

[4] Zhongxin Liu. Study on Microstructure and Properties of GCr15 Bearing Steel by Heat Treatment. Master's Thesis, Hebei University of Science and Technology, Hebei, China, June 2024. [DOI]

[5] Jun Li, Xu Zhang, Hengyong Bu, *et al.* Effects of deep cryogenic treatment on the microstructure evolution, mechanical and thermal fatigue properties of H13 hot work die steel. *Journal of Materials Research and Technology*. 2023, 27: 8100-8118. [Google Scholar] [CrossRef]

[6] Haibo Hu, Lihui Zhu, Youwang Tu, *et al.* Influence of Deep Cryogenic Treatment Process on Microstructure and Properties of M2 High Speed Steel. *Materials Reports*. 2023, 37 (09): 171-176. [DOI] (in Chinese)

[7] Weiting Li, Jun Chai, Geng Liu, *et al.* On the Role of Chemically Heterogeneous Austenite in Cryogenic Toughness of Maraging Steels Manufactured via Laser Powder Bed Fusion. *Acta Materialia*. 2024, 276. [Google Scholar] [CrossRef]

[8] Yuan Ying. Study on austenitizing and cryogenic treatment processof ultra-precision miniature bearing steel balls. Master's Thesis, Hefei University of Technology, Anhui, China. May 2023. [DOI]

[9] Peter Jurči, Ivo Dlouhý. Cryogenic Treatment of Martensitic Steels: Microstructural Fundamentals and Implications for Mechanical Properties and Wear and Corrosion Performance. *Materials*. 2024, 17 (3): 1-78. [Google Scholar] [CrossRef]

[10] Hongyan Wu, Dongxiu Han, Du Yu, *et al.* Effect of Initial Spheroidizing Microstructure after Quenching and Tempering on Wear and Contact Fatigue Properties of GCr15 Bearing Steel. *Materials Today Communications*. 2022, 30. [Google Scholar] [CrossRef]

[11] Zhipeng Gong, Tiantian He, Linfang Li, *et al.* Effect of retained austenite content on friction and wear properties of GCr15 bearing steel. *Transactions of Materials and Heat Treatment*. 2023, 44 (5): 123-134. [Google Scholar] [DOI] (in Chinese)

[12] Yeqing Chen, Yiwen Wu, Ziwei Qin, *et al.* Effect of Deep Cryogenic Treatment on Microstructure and Mechanical Properties of GCr15. *Materials for Mechanical Engineering*. 2018, 42 (5): 55-58, 62. [DOI] (in Chinese)

[13] Lihu Wang, Feng Shuo, Shengyang Cai, *et al.* Effect of Cryogenic Treatment on Grinding Metamorphic Layer and Service Performance of GCr15 Bearing Steel. *Surface Technology*. 2025, 54 (23): 238-252. [DOI] (in Chinese)

[14] Peihong Jiang, Weiye Chen, *et al.* Effects of Holding Time on Microstructure and Properties of Deep Cryogenic Treatment Steel. *Hot Working Technology*. 2018, 47 (14): 155-157. [DOI] (in Chinese)

[15] Zhi Chen, Yu Meng, Dongsheng Lan, *et al.* Effect of cryogenic treatment on high temperature wear resistance of M2Al high speed steel. *Heat Treatment of Metals*. 2022, 47 (8): 158-162. [DOI] (in Chinese)

[16] Zhengrong Ai, Hongyan Wu, Kai Yu, *et al.* Effect of Sub-Zero Treatment on Performance of High Speed Steel W6Mo5Cr4V2. *Special Steel*. 2019, 40 (6): 60-64. [DOI] (in Chinese)

[17] Zhenhuan Liu, Yonghan Li, Yang Liu, *et al.* Carbide Evolution Behavior of GCr15 Bearing Steel During Aging Process. *Chinese Journal of Materials Research*. 2024, 38 (2): 130-140. [DOI] (in Chinese)

[18] Shuo Feng, Tengwei Ding, Na Li, *et al.* Effect of Cryogenic Treatment on Bearing Steel andGrinding Surface Quality. *Surface Technology*. 2025, 54 (9): 248-259. [DOI] (in Chinese)

[19] Qiong He, Yonggang Li, Yanqiang Zhu, *et al.* Effect of Cryogenic Treatment on the Wear and Corrosion Resistance of X52 Pipeline Steel. *Surface Technology*. 2024, 53 (8): 74-83. [DOI] (in Chinese)

[20] Jin He, Bin Yang, Yingchu Wang, *et al.* Effect of Cryogenic Treatment Time on Microstructure and Mechanical Properties of a Low-carbon High-alloy Martensite Steel. *Acta Armamentarii*. 2025, 46 (6): 160-166. [DOI] (in Chinese)

[21] Yanshan Mao, Sanming Du, Lihua Fu, *et al.* Effect of Bainite Content of GCr15SiMo Steel on Mechanical and Wear Properties. *Surface Technolog*. 2024, 53 (7): 48-56. [DOI] (in Chinese)

[22] Alican Boztepe, Ridvan Gecu. Influence of Cryogenic Treatment and Tempering Temperature on Microstructural Evolution and Dry Sliding Wear Behavior of AISI D3 Cold-Work Tool Steel. *Journal of Tribology*. 2025, 147 (6). [Google Scholar] [CrossRef]

[23] Yuan Ren. Effects of Cryogenic Time on Microstructure and Mechanical Properties of 40CrMnNiMo Structural Steel. *Hot Working Technology*. 2022, 51 (2): 142-144. [DOI] (in Chinese)

[24] Mengdan Wang. Effect of Heat Treatment Process on Microstructure and TribologicalProperties of M50 Steel. Master's Thesis, Henan University of Science and Technology, Henan, China, May 2022. [DOI]

[25] Zhiyan Cheng, Liuwei Zheng. Effect of cryogenic treatment on mechanical properties and wear behavior of NM500 wear resistant steel. *China Metallurgy*. 2020, 30 (12): 65-71. [Google Scholar] [DOI] (in Chinese)

[26] Zan Li, Peng Liu, Yinzhe Yang, *et al.* Effect of Rare Earth Treatment on the Friction and Wear Property of Bainite/Martensite Bearing Steel. *Acta Metallurgica Sinica*. 2025, 34 (05): 1-19. [Google Scholar] [DOI] (in Chinese)